

Nucleation in Emulsion Polymerization: A New Experimental Study. 1. Surfactant-Free Emulsion Polymerization of Styrene

I. Kühn and K. Tauer*

Max-Planck-Institut für Kolloid- und Grenzflächenforschung, Kantstrasse 55,
14513 Teltow-Seehof, Germany

Received May 22, 1995; Revised Manuscript Received September 14, 1995*

ABSTRACT: The very early stages of the emulsifier-free emulsion polymerization of styrene were investigated by on-line monitoring of the optical transmission and the conductivity of the reaction mixture. Very careful degassing of the reaction mixture is crucial to achieve high reproducibility. The higher the residual gas concentration the poorer the reproducibility no matter if the gas is air or nitrogen. The results lead to the conclusions that for particle nucleation the rate of initiation in the water phase is very important and that nucleation occurs via cluster formation of water-born oligomers. With the experimental techniques employed, it was possible to investigate the conversion range from 0.47% to 1.8%. However, it was not possible to detect a particle number maximum. Instead of a maximum, a decrease in the particle number was observed followed by a leveling and another increase, indicating another nucleation step.

Introduction

The period of particle formation is probably the most important reaction step but also a very complex process in emulsion polymerization. During the last decades several models have been developed to describe particle nucleation, as for instance, micellar nucleation,^{1,2} homogeneous nucleation,^{3–5} or homogeneous coagulative nucleation.^{6,7} However, with the experimental data available today it is not possible to refute or to confirm any one of these models. All models are largely based on experimental data obtained after the initial particle nucleation period, i.e. at already fairly high conversions of several percent. The crucial point is that no experimental data are available for complete particle number time curves, e.g. from the first appearance of particles up to the end of the polymerization.

The radical polymerization kinetics with an additional assumption regarding the radical capture by micelles or particles as well as assumptions regarding the radical exit form an essential component of these models. For homogeneous nucleation models it is assumed that nucleation occurs when the chain length of the water soluble oligomer radical, j , has reached a critical value, j_{crit} . A value of $j > j_{crit}$ leads to the precipitation of the now water insoluble oligomeric chain as particle or precursor particle. Contrary to this picture, in the micellar nucleation mechanism a primary free radical or an oligomeric radical, both formed in water, enters a monomer-swollen micelle and continues to grow. A particle is formed when a radical starts or continues to grow inside a micelle. Thus, it should take less time to form the first particles via micellar, rather than homogeneous nucleation.

The aim of this paper is to describe a new experimental approach to investigate the very early stages of emulsion polymerization to obtain reliable experimental data. The very early stages means a polymer content in the range from zero to approximately 1%. Indeed, the experimental results reported here make it clear that the experimental setup allows the monitoring of the onset of particle formation.

Experimental Part

Chemicals. Styrene (Sigma Aldrich) was purified by standard procedures to remove stabilizers, distilled under vacuum, and stored in a refrigerator until use. The initiator potassium peroxydisulfate (PPS, Riedel-de Haën) with 99% purity, sodium dodecyl sulfate (Sigma) with 99% purity, and the radical scavenger sodium nitrites (Aldrich) with 97% purity were used as received. Deionized water from an ion exchanger was fed to a REWA HQ5 apparatus for high end purification. REWA HQ5 is a combination of UV treatment to destroy germs, an adsorption cartridge to remove organic impurities, a special ion exchanger, and depth filters followed by membrane filters for microfiltration. The quality was checked by conductivity measurement and surface tension. The water was used when the conductivity was below $0.5 \mu\text{S cm}^{-1}$ (at 333 K) and the surface tension above 72 mN m^{-1} .

Reactor. All polymerizations were carried out in a specially constructed Teflon reactor of 400 mL reaction volume equipped with a stirrer, nitrogen inlet and outlet, sensors for on-line measurement of the reactors inside temperature and conductivity, and two optical windows for an on-line monitoring of the optical transmission (Figure 1). The optical path through the reactor is 9.8 cm. This is fairly high, but is the main reason for the high sensitivity of the detection system. An additional opening in the reactor top allows for injecting reactants such as, for instance, initiator solution to start the polymerization as well as for taking samples from the reaction mixture for off-line analysis.

The conductivity and the temperature of the reaction mixture were measured with a conductivity meter CDM83 from Radiometer, Copenhagen, equipped with a PP1042 conductivity electrode and a T801 temperature sensor. The optical transmission was measured at a wavelength of 546 nm (green mercury line) with an optical spectrophotometer SPE-KOL 11 from Carl Zeiss Jena. A data acquisition module was written in PASCAL to collect values for temperature, electrical conductivity, and optical transmission every 6 s on a personal computer. Furthermore, the time curves of these quantities are displayed on-line on the PC screen for reaction control, and for selecting interesting points of the transmission curve to take samples for off-line analysis.

Monomer Feed to the Reaction Mixture. A crucial point for on-line monitoring of an emulsion polymerization with optical transmission measurement is to avoid monomer droplets as well as gas bubbles in the reaction mixture. On the other hand the monomer feed must be high enough to start and subsequently to maintain the polymerization reaction.

At first different types of Teflon cylinders were used as monomer reservoirs (cf. Figure 2). Both ends of the cylinders were capped with membranes to separate the monomer and

* Abstract published in *Advance ACS Abstracts*, November 1, 1995.

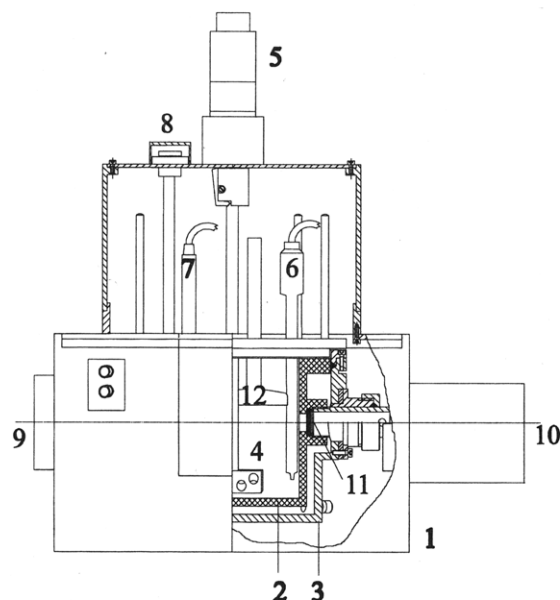


Figure 1. Profile section of the reactor adapted to the spectrometer SPEKOL 11: 1, case; 2, Teflon reactor; 3, Teflon jacket; 4, stirrer; 5, electric motor; 6, conductivity probe; 7, temperature probe; 8, sample injection tube; 9, photomultiplier; 10, light source (SPEKOL 11); 11, glass window; 12, funnel.

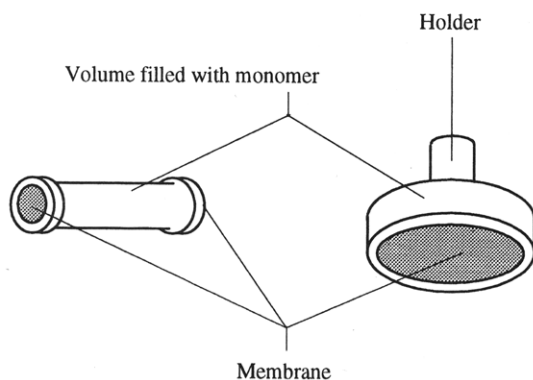


Figure 2. Schematic drawing of different types of monomer reservoirs tested.

water phases. This construction worked fairly well, however with some essential drawbacks and difficulties. These are, with respect to material and pore size, the selection of a proper membrane, sometimes mechanical instabilities of the membrane, and an impurity layoff. Finally, this procedure resulted in a poor reproducibility caused by a combination of all of these problems.

A funnel staying underwater with its wide side being only 3 mm proved to be the best way to ensure a constant and highly reproducible monomer feed to the reaction mixture (cf. number 12 in Figure 1). With this simple arrangement one can realize a constant interface for monomer diffusion during the whole polymerization time. It is important to adjust the stirring carefully to avoid breakage of the monomer phase under the glass funnel.

Preparation of the Reaction Mixture. For a first series of polymerizations oxygen was removed from water and monomer by bubbling nitrogen through the liquids at ambient temperature. However, the reproducibility obtained with this procedure was poor (cf. Figure 3). It turned out that the prevention of bubble formation during the reaction is crucial for reproducibility. This was achieved by degassing under vacuum and elevated temperature. At a temperature slightly above the reaction temperature the reactor was filled with water. The monomer was always degassed by a vacuum treatment. The reproducibility was greatly enhanced by this procedure (cf. Figure 4).

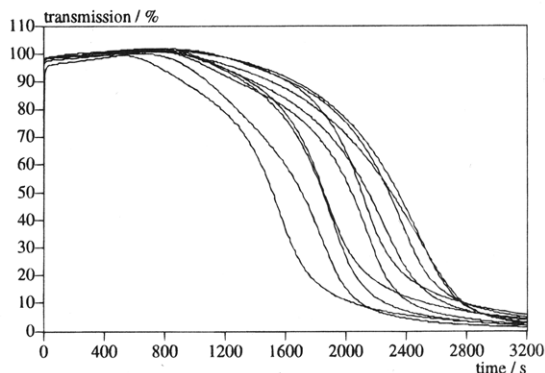


Figure 3. Illustration of the bad reproducibility if water and monomer are only pretreated by bubbling nitrogen through the liquids (degassing procedure D) at ambient temperature; run I2.

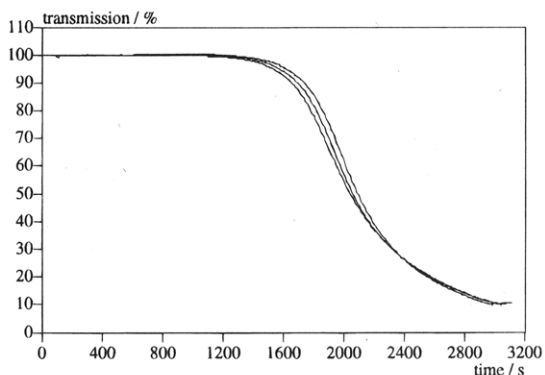


Figure 4. Illustration of the drastically enhanced reproducibility if the water is degassed under vacuum, afterward heated while nitrogen is bubbled through, then degassed again under vacuum, and fed into the reactor at a temperature higher than the reaction temperature (degassing procedure A); run I2.

Table 1. Polymerization Conditions (Concentrations Based on Total Water Volume)

run	PPS (mM)	temp (°C)	R_i (mol L ⁻¹ s ⁻¹)
I1	1.25	60	3.7×10^{-9}
I2	2.50	60	7.4×10^{-9}
I3	3.75	60	1.1×10^{-8}
I4	5.00	60	1.5×10^{-8}
I2	2.50	60	7.4×10^{-9}
T2	2.50	65	1.6×10^{-8}
T3	2.50	70	3.2×10^{-8}
T4	2.50	80	1.3×10^{-7}

constant conditions styrene 5 mL (4.3×10^{-2} mol)
 total water 400 mL (22.22 mol)
 stirrer speed 160 rpm

^a Styrene volume under the funnel.

Polymerization. All polymerizations were carried out emulsifier free, i.e. without added emulsifier. Various radical fluxes, R_i , were produced by variation of the polymerization temperature and initiator concentration, respectively (cf. Table 1). The radical flux was calculated according to (1) with $k_d =$

$$R_i = 2fk_d I_0 \quad (1)$$

$4.8 \times 10^{16} e^{-16869.243/T}$ and $f = 0.3$,⁹ where k_d is the initiator decomposition rate constant, T is the absolute temperature, I_0 is the initial initiator concentration, and f is the primary radical efficiency.

The reactor was filled with degassed water (390 mL), and the monomer was placed in the funnel. After that, the closed reactor was thermostated. After an equilibration time of at least 2 h the reaction was started by injecting the corresponding amount of initiator dissolved in 10 mL of degassed water. During the equilibration the optical transmission remains

constant. The stability of the optical system was tested in blank runs with water and monomer but without initiator. It was found that the transmission decreased under these conditions from 100% to 98.7% after 16 h. At the desired final transmission the polymerization was stopped by charging with a syringe 20 mL of a solution containing 0.105 M sodium nitrite an 0.315 M sodium dodecyl sulfate to the reaction mixture. Furthermore, samples were taken from the reactor at different transmissions for off-line analysis. These samples with a volume of 0.5 mL were immediately mixed with 0.2 mL of a solution containing 0.1 M sodium nitrite to stop polymerization and 4.93 mM sodium dodecyl sulfate to prevent coagulation. The results reported on here are average values from at least three polymerizations.

Latex Characterization. Latex samples were taken from the reactor at different times (transmission values) for an off-line particle size distribution analysis by dynamic light scattering (DLS) and transmission electron microscopy (TEM). Dynamic light scattering measurements were done with a NICOMP particle sizer, Model 370. The measurements have been carried out as long as at least 3×10^5 counts have been accumulated in channel 1 for a sufficient statistical certainty. Besides the PSD, the volume-weighted diameter was used for further calculations. For TEM investigations a few microliters of the latex was dropped on a collodium-coated copper grid and dried at ambient temperature. After that, the particles were shadowed with a Pt-Ir-C alloy to enhance the contrast. Micrographs were obtained on a TESLA BS 500 transmission electron microscope at an acceleration voltage of 60 kV. The particle size distributions were determined by counting at least 700 particles per sample with an OPTON TGZ3 counter.

From the PSD measured by TEM the root-mean-cube particle diameter (D_{rmc}) was estimated, which is the appropriate average to calculate particle numbers.¹⁰

Results and Discussion

Theory. Particle formation in emulsion polymerization is a very fast process. Therefore, an on-line measurement with high-speed data acquisition and a good data resolution is needed. As well, the technique employed should not influence the nucleation process and must be easy to perform. The turbidimetric method fulfills all of these conditions.

Characterization of latexes by turbidity measurements has been developed by Wallach,¹¹ Lange,¹² and Zollars.¹³ Zollars¹³ described also an on-line application of these techniques.

The turbidity τ can be calculated from (2), where l is the optical path length, I_0 is the incident light intensity, and I is the light intensity after passing through the polymerization mixture.

$$\tau = \frac{1}{l} \ln \frac{I_0}{I} \quad (2)$$

For a monodisperse system of nonabsorbing particles, assuming single point scattering, the specific turbidity is given according to Mie¹⁴ by (3). λ is the wavelength

$$\left(\frac{\tau}{C}\right)_{C \rightarrow 0} = \frac{4\pi n_0}{\lambda \rho_T} f(\alpha, m) \quad (3)$$

$$\alpha = \frac{\pi D_T n_0}{\lambda} \quad m = \frac{n_D}{n_0}$$

of the incident light, n_D and n_0 are the refractive indexes of the spheres and of the medium, C is the polymer concentration, D_T is the diameter of the particle, and ρ is the polymer density.

For small particles ($0 < \alpha \lesssim 1$) and low relative refraction indexes ($1 < m \lesssim 1.3$) the function $f(\alpha, m)$ can

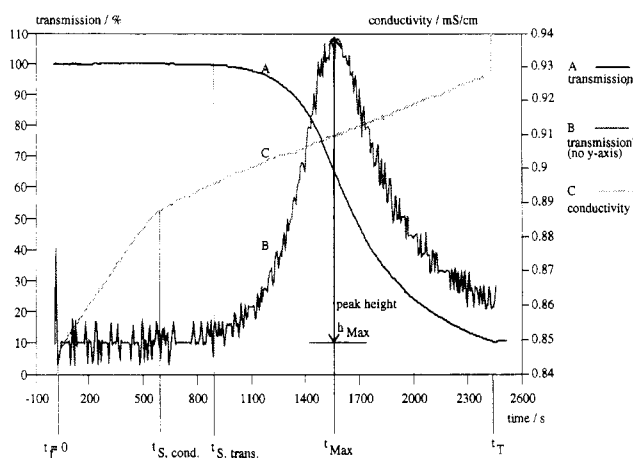


Figure 5. Illustration of characteristic quantities to evaluate the experiments; run I2.

be approximated by (4). Usually, (4) is a very poor

$$f(\alpha, m) = \left(\frac{m^2 - 1}{m^2 + 2}\right)^2 \alpha^3 \quad (4)$$

approximation. However one can use it under the special experimental conditions, as shown by an example. For a specific turbidity of $\tau/c = 0.2 \text{ L/(g/cm)}$ (a typical value representing the experimental conditions) the tables of scattering functions¹⁷ give a particle diameter of $D_T = 45.65 \text{ nm}$ whereas (4) gives a value of $D_T = 45.98 \text{ nm}$.

For this estimation the following values have been used: wavelength $\lambda = 546 \text{ nm}$, relative refraction index of polystyrene/water at 546 nm $m_{\text{polystyrene/water}} = 1.203$ (α is always $\lesssim 1$ if the particle diameter is $\lesssim 130 \text{ nm}$). The difference of 0.33 nm is really negligible.

In any other case the diameter of colloidal spheres can be determined by numerical computations of the light scattering functions from the Mie theory.^{15,16}

Specially, the tables of scattering functions for spherical particles published by Verner¹⁷ were used. If turbidity and particle diameter are known, these tables can be used in the reverse sense to calculate the polymer concentration.

Another way to estimate the polymer concentration would be to use elemental analysis data for C and S of the solid. Hence, one knows the amount of sulfur brought into the solid by lauryl sulfate and persulfate and can then calculate the amount of polymer formed. However, the error is fairly high since the polymer concentration is very low, on the order of 0.1 g L^{-1} .

Knowing the particle size from dynamic light scattering or TEM and the polymer concentration from turbidity data, one can now estimate the particle number according to (5).

$$N = \frac{C}{\rho \frac{\pi}{6} D^3} \quad (5)$$

Experimental Results. Figure 5 shows a typical set of results. As can be seen, the reaction can be characterized by the following quantities: initiator injection time (t_I), two times indicating possibly the onset of particle nucleation ($t_{S, \text{trans}}$ from the transmission time curve and $t_{S, \text{cond}}$ from the conductivity time curve), at least one time for a point of inflection in the transmission time curve or the maximum of its first derivative

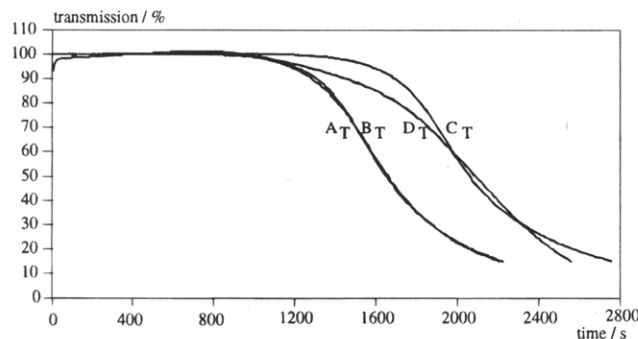


Figure 6. Influence of different degassing procedures on the course of the reaction; run I2. Indexes C and T refer to conductivity and transmission, respectively. (A) Vacuum treatment followed by boiling and another vacuum treatment. The reactor was filled with hot water with a temperature a little bit higher than the reaction temperature. (B) Nitrogen was bubbled through boiling water for 1 h, and then the reactor was filled with the hot water. (C) Same procedure as B, but the reactor was filled with cold water. (D) Nitrogen was bubbled through cold water for 1 h.

Table 2. Illustration of Reproducibility of the Characteristic Observables

	av + std	
	degassing A	degassing D
$t_{S,cond}$ (s)	$549.7 \pm 4.27\%$	$586.0 \pm 18.5\%$
$t_{S,trans}$ (s)	$740.0 \pm 4.46\%$	$804.0 \pm 9.1\%$
t_{Max} (s)	$1516.0 \pm 2.86\%$	$2211.0 \pm 11.0\%$
h_{Max} (% s ⁻¹)	$-0.1394 \pm 2.15\%$	$-0.137 \pm 16.9\%$

(transmission') with respect to time (t_{Max}), the height of the maximum (h_{Max}), and the injection time of the radical scavenger (t_T) which corresponds to the end of the polymerization.

The decrease in transmission (or the increase in turbidity) is a complex function of particle number and diameter. It could be due to an increase in particle concentration, N , or if N remains unchanged due to the particle growth.

Conductivity measurement is a useful tool to differentiate between homogeneous and micellar particle nucleation in mini emulsion polymerization.¹⁸ The results presented here confirm the suitability of conductivity measurement to obtain information concerning particle nucleation in emulsifier-free emulsion polymerization, too. Another useful on-line method is transmission measurement, as also shown in Figure 5.

The various attempts to find a suitable pretreatment of all ingredients made it clear that residual dissolved gas in the reaction mixture is detrimental, regardless of whether the gas is air or nitrogen.¹⁹ Lowering of the gas concentration leads to an earlier decrease in the turbidity as well as in the slope of the conductivity time curve. These results are illustrated in Figure 6 by means of average curves for different kinds of degassing the reaction water. The transmission time curves for degassing procedures A and B are the same, but both are distinctly different from C as well as from D.

Table 2 further illustrates the differences in dependence on the gas concentration. The only one characteristic quantity that has the same average value, i.e. which does not depend on the gas concentration, is h_{Max} . This is noteworthy since h_{Max} corresponds to an overall reaction rate (more precisely the maximum of the rate) in which all reactions are included, leading to an increase in turbidity.

It is conspicuous that the standard deviations for the runs with the lowest gas concentration are by a factor

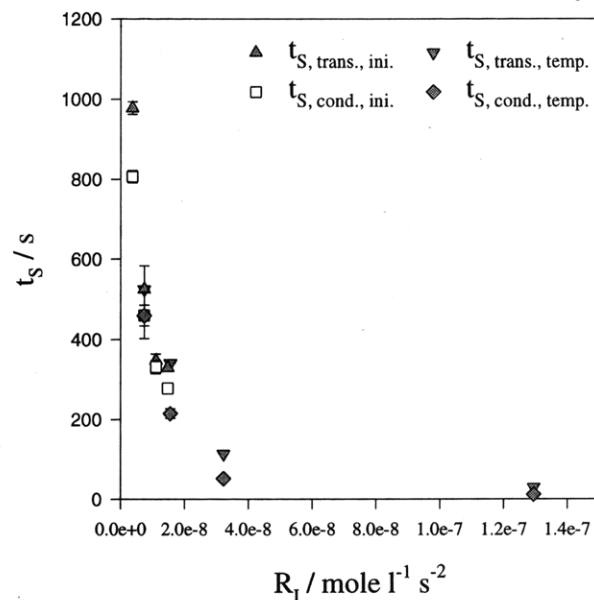


Figure 7. Dependence of $t_{s,cond}$ and $t_{s,trans}$ on R_i . $t_{s,trans,ini}$ = time corresponding to the start of transmission decrease depending on R_i ; runs in which R_i is altered by changing I_0 . $t_{s,trans,temp}$ = time corresponding to the start of transmission decrease depending on R_i ; runs in which R_i is altered by changing temperature. $t_{s,cond,ini}$ = time corresponding to the change in conductivity slope depending on R_i ; runs in which R_i is altered by changing I_0 . $t_{s,cond,temp}$ = time corresponding to the change in conductivity slope depending on R_i ; runs in which R_i is altered by changing temperature.

of up to 8 smaller than those from the runs with the highest gas concentration. The reproducibility during the nucleation period of a dispersion polymerization is also reported to be fairly poor.²⁰ However, the experimental results presented here prove the influence of the kind of degassing of the reaction mixtures (or the gas concentration in the reaction water) on particle nucleation. Degassing as much as possible leads to a drastically enhanced reproducibility also in the very early stages of emulsion polymerization.

Furthermore, it is clearly seen from Figure 5 and Table 2 that conductivity and transmission respond to nucleation at different times after initiation. The slope in the conductivity curve changes first followed by a decrease in transmission. This seems to be reasonable within the picture of homogeneous nucleation corresponding to classical nucleation theory.²¹ According to this model, cluster formation of water soluble oligomers before nucleation should lead to a decrease in conductivity but should not yet change transmission. The clusters are not yet particles since they can redissociate again. The decrease in transmission is due to the existence of larger particles. So, the nucleation time is very likely between $t_{s,cond}$ and $t_{s,trans}$.

Furthermore, the similarity in the dependence of $t_{s,cond}$ and $t_{s,trans}$ on the radical flux leads to the conclusion that both quantities describe a similar event (cf. Figure 7). One must bear in mind that an increasing initiator concentration and/or an increasing temperature leads to an increasing radical flux. Additionally, an increasing initiator concentration leads to an increase in the ionic strength, too. Obviously, there is no remarkable effect of the ionic strength on both t_s values. All the data points for altering the initiator concentration as well as for altering the temperature follow one curve when the radical flux is considered an independent variable. One would expect a difference between the

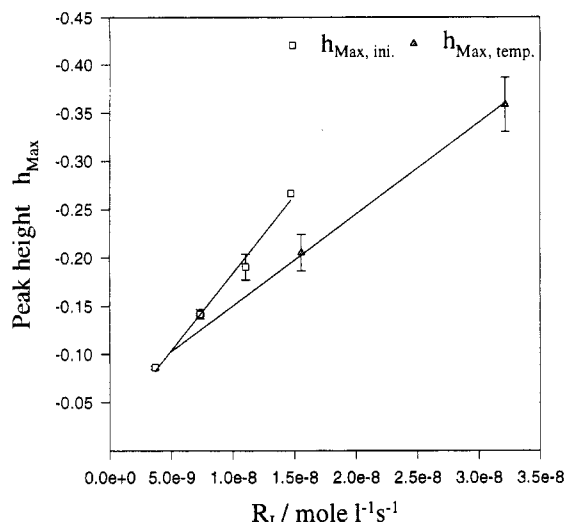


Figure 8. Dependence of h_{Max} on R_i . $h_{\text{Max,ini}} = h_{\text{Max}}$ depending on R_i when R_i is altered by changing I_0 . $h_{\text{Max,temp}} = h_{\text{Max}}$ depending on R_i when R_i is altered by changing temperature.

concentration and the temperature dependence if there were a remarkable influence of the ionic strength on nucleation.

However, a different situation exists after particle formation. Figure 8 shows that the dependence of h_{Max} on R_i is different depending on whether I_0 or T is varied.

For emulsion polymerizations it is well-known that added electrolytes have an influence on the polymerization rate.^{22,23} The effect depends on the particular polymerization conditions. For styrene emulsion polymerization in the presence of potassium dodecanoate the rate accelerates with increasing potassium chloride concentration.²² In contrast, the polymerization rate decreases for a vinyl chloride emulsion polymerization in the presence as well as in the absence of emulsifiers with increasing amounts of sodium chloride.²³

According to the results presented in Figure 8, the overall reaction rate (h_{Max}) is higher for I_0 above 2.5 mM when the radical flux is adjusted by potassium persulfate concentration instead of temperature.

In contrast, the time for reaching the maximum (t_{Max}) follows again only one curve regardless of whether I_0 or T has been used to adjust R_i (Figure 9).

The sample taken at a transmission of 80.9% was the first for which it was possible to measure a particle size distribution by DLS with the NICOMP particle sizer. However, to reach the appropriate statistical certainty, the duration was 8 h caused by the very low scattering intensity. The results summarized in Figure 10 make it clear that both DLS and TEM give similar results concerning the range of particle sizes as well as concerning the change with proceeding polymerization. The differences between TEM and DLS are very likely the result of the uncertainty of DLS measurements due to the low scattering intensity of the samples (standard deviation: DLS \approx 15%, TEM \approx 10%).

A further proof for the similarity of the results obtained with both methods are the results shown in Figure 11. The course of D_v from DLS and of D_{rmc} from TEM with polymerization time is almost the same.

Figure 12 shows that the polymerizations led to very low polymer concentrations of about 0.2 g L⁻¹, corresponding to a monomer conversion of approximately 1.8%. Surprisingly, it was not possible to detect a particle number maximum within the conversion range from 0.47% to 1.8% (which was the range possible to

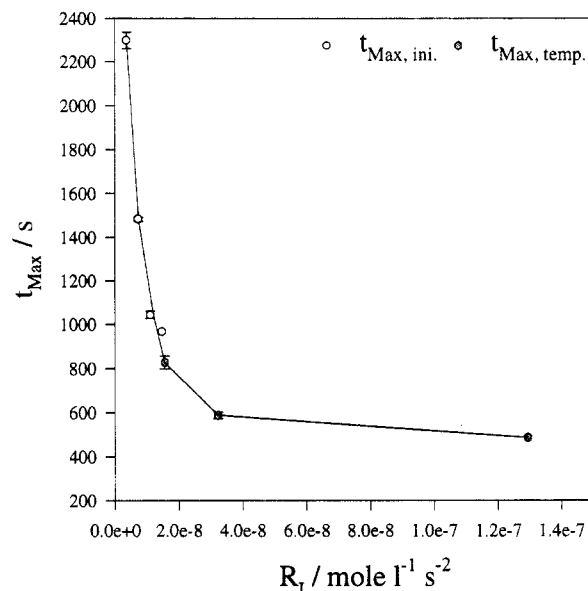


Figure 9. Dependence of t_{Max} on R_i . $t_{\text{Max,ini}} = t_{\text{Max}}$ depending on R_i when R_i is altered by changing I_0 . $t_{\text{Max,temp}} = t_{\text{Max}}$ depending on R_i when R_i is altered by changing temperature.

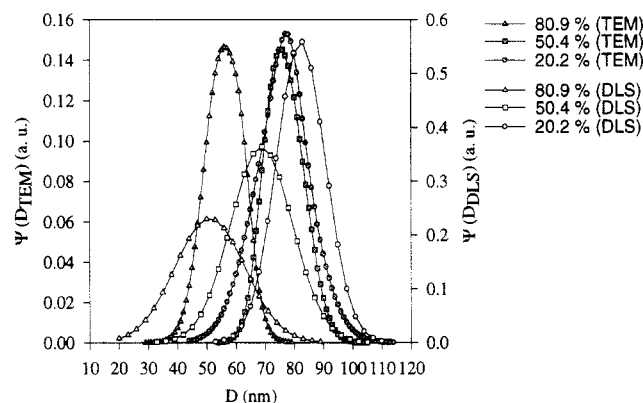


Figure 10. Comparison of the PSD determined with TEM and DLS at different transmission values (polymerization times); run I2.

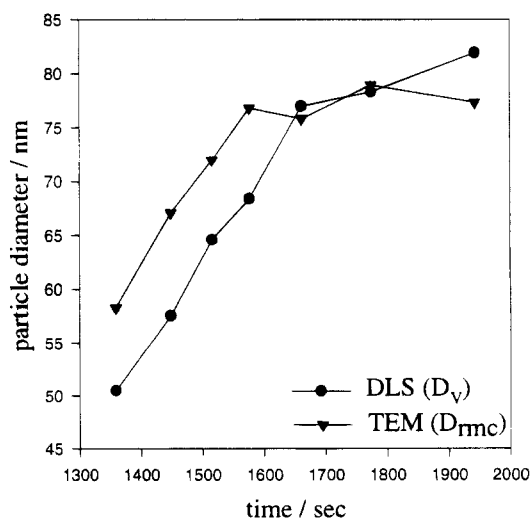


Figure 11. Development of the mean particle diameter with increasing polymerization time (increasing transmission) estimated from DLS and TEM; run I2.

investigate). A decrease in the particle number followed by a leveling and a slight increase has been estimated over the investigated polymerization period. This is the general picture estimated with both techniques em-

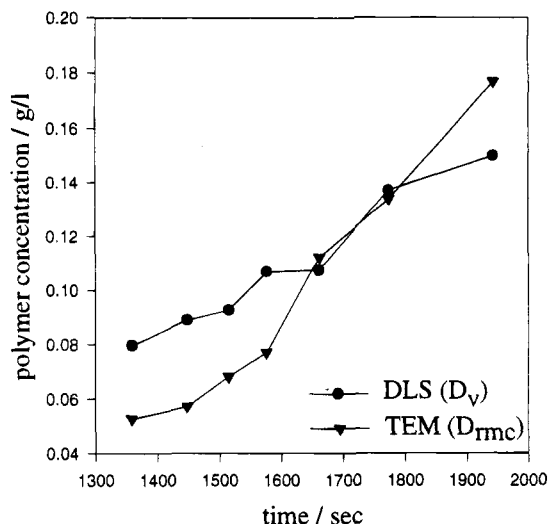


Figure 12. Development of the polymer concentration with polymerization time (increasing transmission) calculated from the turbidity and the mean particle diameter; run I2.

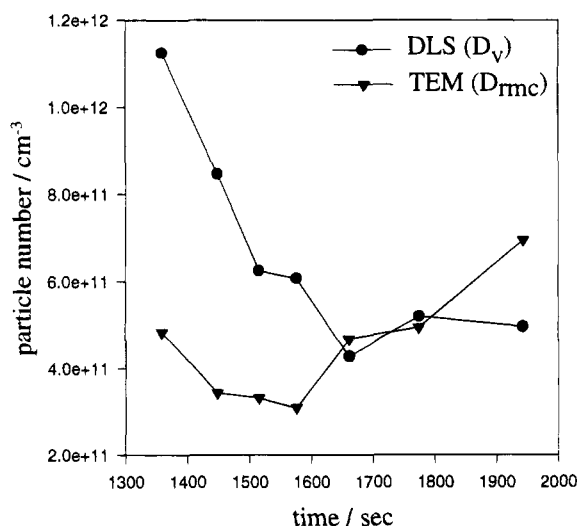


Figure 13. Development of the particle number with polymerization time (increasing transmission); run I2.

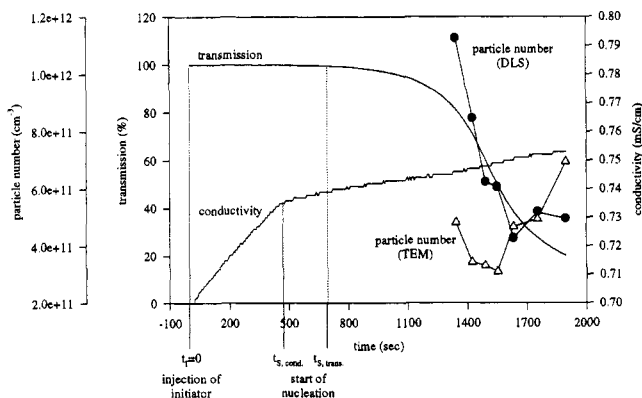


Figure 14. Summary of the results obtained with the different experimental techniques.

ployed for measuring particle sizes (cf. Figure 13). The observed increase in the particle number indicates another particle nucleation step.

Figure 14 summarizes the results obtained during these investigations concerning the different techniques employed. It is reasonable to assume that the nucleation starts at a time that is between that for the bend in the conductivity curve ($t_{s,cond}$) and that for the start

of the transmission decrease ($t_{s,trans}$). However, with the NICOMP particle sizer as well as with the TEM it was not possible to measure in this range of the polymerization particle sizes.

So, the maximum in the particle number time curve must appear at still lower conversions (transmissions). However, if the nucleation process itself is very fast, it could be possible that its time dependence cannot be resolved experimentally and, subsequently, one would measure a sudden jump to a certain particle number. For the emulsifier-free emulsion polymerization it is very likely that just after nucleation the particle number decreases due to the colloidal instability of the very small particles. This is not unusual, since Goodall et al.²⁴ observed also a decreasing particle number followed by a leveling, again without the detection of a maximum, for the emulsifier-free emulsion polymerization of styrene. Also, for other monomers in the absence as well as in the presence of emulsifier below and above the critical micelle concentration a decrease in the particle number has been detected.²⁵⁻²⁷

Goodall et al.²⁴ have done their investigations with a recipe and a procedure leading to approximately 90% conversion and ca. 7% solid content of the final latexes. However, they obtained particle numbers in the range between 10^{12} and 10^{11} cm⁻³, as is also the case for the system investigated here (cf. Figure 13).

Summary

Results are presented concerning the particle nucleation in the emulsifier free emulsion polymerization of styrene by an on-line monitoring of both optical transmission and conductivity during the very early stages of the polymerization, up to a monomer conversion of 2%. Very careful degassing of the reaction mixture turned out to be crucial to achieve high reproducibility. The higher the gas concentration the poorer the reproducibility, no matter if the gas is air or nitrogen.

The results make it clear that for particle nucleation the rate of initiation in the water phase is very important. Furthermore, it makes no difference if R_i is adjusted by the initiator concentration or by the temperature. These results indicate that there is no electrolyte influence on nucleation.

From a bend in the conductivity time curve that occurs before the transmission starts to decrease, it is concluded that the nucleation occurs via cluster formation of water-born oligomers.

With the experimental techniques employed for measuring the particle size, it was possible to investigate the conversion range from 0.47% to 1.8%. However, it was not possible to detect a particle number maximum in this range. The particle number decreases in a first period, then stays constant, and increases again, indicating another particle nucleation step.

References and Notes

- (1) Harkins, W. D. *J. Am. Chem. Soc.* **1947**, *69*, 1428.
- (2) Smith, W. V.; Ewart, R. H. *J. Chem. Phys.* **1948**, *16*, 592.
- (3) Priest, W. J. *J. Phys. Chem.* **1952**, *56*, 1077.
- (4) Fitch, R. M.; Tsai, C. H. In *Polymer Colloids*; Fitch, R. M., Ed.; Plenum Press: New York, 1971; p 73.
- (5) Hansen, F. K.; Ugelstad, J. In *Emulsion Polymerization*; Academic Press: New York, 1982.
- (6) Lichti, G.; Gilbert, R. G.; Napper, D. H. *J. Polym. Sci., Part A: Polym. Chem.* **1983**, *21*, 269.
- (7) Feeney, P. J.; Napper, D. H.; Gilbert, R. G. *Macromolecules* **1976**, *9*, 536.
- (8) Henrice-Olive, G.; Olive, S. In *Chemische Taschenbücher 8*; Verlag Chemie: Berlin, 1969; p 7.

- (9) Song, Z.; Poehlein, G. W. *J. Colloid Interface Sci.* **1989**, *128*, 483.
- (10) Gardon, J. L. *J. Polym. Sci., Part A: Polym. Chem.* **1968**, *6*, 643.
- (11) Wallach, L. D.; Heller, W.; Stevenson, A. F. *J. Chem. Phys.* **1961**, *32* (5), 1796.
- (12) Lange, H. *Colloid Polym. Sci.* **1968**, *223* (1), 24.
- (13) Zollars, R. L. *J. Colloid Interface Sci.* **1980**, *74* (1), 163.
- (14) Mie, G. *Ann. Phys.* **1908**, *25*, 377.
- (15) Heller, W.; Pangonis, W. *J. Chem. Phys.* **1957**, *26* (3), 498.
- (16) Heller, W. *J. Chem. Phys.* **1957**, *26*, 920.
- (17) Verner, B.; Bárta, M.; Sedláček, B. *Tables of scattering functions for spherical particles*; Edice Macro: Prague, 1976.
- (18) Wang, I.; Schork, F. J. *J. Appl. Polym. Sci.* **1994**, *54*, 2157.
- (19) The authors are grateful to B. W. Ninham for hints regarding a possible influence of gas dissolved in the reaction mixture.
- (20) Shen, S.; Sudal, E. D.; El-Aasser, M. S. *J. Polym. Sci., Part A: Polym. Chem.* **1992**, *32*, 1087.
- (21) Tauer, K.; Kühn, I. *Macromolecules* **1995**, *28*, 2236.
- (22) Said, Z. F. M. *Polym. Int.* **1994**, *35*, 379.
- (23) Neelsen, J.; Jaeger, W.; Tauer, K.; Hecht, P. *Acta Polym.* **1985**, *36*, 694.
- (24) Goodall, A. R.; Wilkinson, M. C.; Hearn, J. J. *Polym. Sci., Part A: Polym. Chem.* **1977**, *15*, 2193.
- (25) Hergeth, W.-D.; Lebek, W.; Kakuschke, R.; Schmutzler, K. *Makromol. Chem.* **1991**, *192*, 2265.
- (26) Tauer, K.; Paulke, B.-R.; Müller, I.; Jaeger, W.; Reinisch, G. *Acta Polym.* **1982**, *33*, 287.
- (27) Tauer, K.; Neelsen, J.; Hellmich, C. *Acta Polym.* **1985**, *36*, 665.

MA950694+